5-axis double-flank CNC machining of spiral bevel gears via custom-shaped tools – Part II: physical validations and experiments

Gaizka Gómez Escudero*,a, Pengbo Bo^b, Haizea González^a, Amaia Calleja^a, Michael Bartoň^c,d, Luis Norberto López de Lacalle^a

^a High Performance Manufacturing Group, Department of Mechanical Engineering,
the University of the Basque Country, Plaza Ingeniero Torres Quevedo 1, 48013, Bilbao, Basque Country, Spain
^b School of Computer Science and Technology, Harbin Institute of Technology, West Wenhua Street 2, 264209 Weihai, China
^c BCAM – Basque Center for Applied Mathematics, Alameda de Mazarredo 14, 48009 Bilbao, Basque Country, Spain
^d Ikerbasque – Basque Foundation for Sciences, Maria Diaz de Haro 3, 48013 Bilbao, Basque Country, Spain

Abstract

Recently, a new methodology for 5-axis flank computer numerically controlled (CNC) machining, called *double-flank* machining, has been introduced (see "5-axis double-flank CNC machining of spiral bevel gears via custom-shaped milling tools–Part I: Modeling and simulation"). Certain geometries, such as curved teeth of spiral bevel gear, admit this approach where the machining tool has tangential contact with the material block on two sides, yielding a more efficient variant of flank machining. To achieve high machining accuracy, the path-planning algorithm, however, does not look only for the path of the tool, but also for the shape of the tool itself. The proposed approach is validated by series of physical experiments using an abrasive custom-shaped tool specifically designed for a particular type of a spiral bevel gear. The potential of this new methodology is shown in the semifinishing stage of gear manufacturing, where it outperforms traditional ball end milling by an order of magnitude in terms of machining time, while keeping, or even improving, the machining error.

Key words: 5-axis CNC machining, double-flank machining, custom-shaped tools, semifinishing operations, tangential movability, free-form shape manufacturing

1. Introduction

Efficient and highly-accurate manufacturing of curved geometries such as car transmissions, gearboxes, or other doubly-curved engine parts is a serious challenge in many industries like automotive or aeronautic, to name a few. Spiral bevel gears, when compared to straight-toothed bevel gears, are able to run at higher speed [1] and are therefore indispensable elements among gear mechanisms. To achieve smooth and silent high-speed transmission, manufacturing with a very high precision is essential, e.g. using direct face nanogrinding [2]. Moreover, high precision increases durability of the manufactured gears that is another main objective for modern, sustainable manufacturing technologies [3].

Traditionally, manufacturing of spiral bevel gears requires specially-deviced machines. There are several mainstream approaches to manufacture spiral bevel gears: gear hobbing with perimeter cut (Gleason) [4], cyclo-palloidal continuous generation by spiral hobbing (Klingelnberg and Oerlikon) [5], and continuous generation by spiral hobbing with conical-type cut (Klingelnberg) [1]. However, all these approaches are appropriate for large manufacturing batches.

In contrast, the proposed approach aims at low-cost manufacturing of a single workpiece and/or replacement of a broken part using 5-axis computer numerically controlled (CNC) machining. The recent trends in gear manufacturing already head this direction [6, 7, 8], which is well-suited for small batches and an economical alternative to the traditional approach using an expensive hobbing machine. At the same time, CNC machining is able to keep high-accuracy that is essential for gear manufacturing. Another significant advantage of 5-axis CNC machining comes from the fact that it can be combined with additive manufacturing [9]. This type of *hybrid manufacturing* enables, for example, gear repair, that is something highly desirable, but not possible with the traditional gear-cutting methods.

The purpose of this study is to further advance the recent geometric modeling simulations on 5-axis CNC machining with custom-shaped tools [10]. That is, the path-planning algorithm does not only look for optimal machining paths, but also for the shape of the tool itself [11, 12, 13]. While flank milling with curved (barrel) tools is known and possible for input free-form surfaces [14, 10] simultaneous tangential contact on two sides requires a specific input geometry. The recent numerical simulation results showed that for spiral bevel gears, a custom-shaped tool admits enough freedom to flank-machine a curved valley between two spiral gear teeth with a single sweep, having a bi-tangential contact throughout the motion. This newly introduced methodology, called *double-flank*, therefore offers even more efficient manufacturing than traditional flank ma-

---
*Corresponding author
Email addresses: gaizka.gomez@ehu.eus (Gaizka Gómez Escudero), pbbo@hit.edu.cn (Pengbo Bo), haizea.gonzalez@ehu.eus (Haizea González), amaia.calleja@ehu.eus (Amaia Calleja), mbarton@bcamath.org (Michael Bartoň), norberto.lzlacalle@ehu.eus (Luis Norberto López de Lacalle)

1

chining. On a conceptual level, the tools used in this work are very similar to small grinding wheels [15, 16, 17], i.e., metal cores coated with abrasive particles [18, 19]. Therefore, the effects of the abrasive grains on the surface have to be taken into consideration.

In this paper, real machining experiments are conducted to physically validate the recently proposed double-flank machining methodology. The results show that this approach outperforms classical ball-end milling by order of magnitude in terms of machining time and, for the particular spiral bevel gear considered in this paper, this approach is well-suited for the semi-finishing stage. The results are also virtually compared against (single) flank machining with on-market barrel tools with favorable results for the proposed double-flank machining with custom-shaped tools.

2. Previous work

Manufacturing of spiral bevel gears has been studied over several past decades, see e.g. [1, 4, 5, 20] and other relevant references in [20]. The whole loop: design, production, inspection and installation of spiral-toothed bevel gears is a complex process that requires a special treatment. There are several geometric constraints that need to be satisfied to guarantee smooth transmission between the cutting tool and the material block: (i) the flank contact between the conjugate gear pair (the tool and tooth) has to be along a whole line (curve), (ii) the line contact is equally distributed in the entire engagement area, and (iii) the line contact needs to preserved at every instant of the motion [4].

Traditional pipeline for manufacturing of gears is aimed for large batches and groove-making machines that rely on slotting on curved tool. The two main approaches: the continuous indexing method, referred to as "face hobbing", and the single indexing method referred to as "face milling" present some differences. The face hobbing method produces an epicycloidal shape in tooth lengthwise direction. The face milling method is processed in such a way that both flanks are manufactured in a single cut, i.e., a constant slot width results in the tooth root due to the circular cutter head [21]. While palloid gears are produced by a conical hob, the cyclo-palloid gears are manufactured using a face hob cutter.

This paper belongs to a family of modern approaches that focus on gears manufacturing using universal multitasking machines or five-axis milling centers [22, 23]. The main advantage of this new trend stems in its versatility as the tool in general does not depend on the gear geometry. This fact makes the technology very flexible as it can be performed on various milling centers, and not, in contrast to the traditional methods (Gleason and Klingelnberg), on one specific large-scale machine.

Suh et al. [8] use a 3-axis milling machine with a rotary table, however, ball end milling is applied in semi-finishing and finishing stages. A numerical approach for determination of machine-tool settings for roughing of a pinion by using a spread-blade face-milling cutter is proposed in [3]. Five-cut method is applied and the manufacturing time is minimized by maximizing the material cut during the rough-cutting stage.

Traditionally, standard tools are frequently used for gears machining in universal machining centers [7]. However, this paper follows the recent trend where free-form tools are used for near-to-net-shape machining, especially for complex slots, such as the tooth space of the gear.

For certain type of gears, such as non-circular spur bevel gear, the irregular shape makes the design and manufacturing process even more difficult and forging stage is involved to distribute the material according to the shape features of the gear [24]. Another issue that needs to be carefully considered is surface roughness. A model to predict and control the teeth surface roughness for 3+2 axis milling using ball-end milling has been proposed recently [25].

Other recent works have focused on gears machining with universal machines using milling technology [26, 27]. However, innovative processes with higher material removal rates are one of the main objectives in modern manufacturing. In this line, Super Abrasive Machining (SAM) [28] is one versatile and feasible solution that increases gears' machining efficiency. Specifically, SAM provides grinding technology precision [29] with similar machining feeds and costs, but with shorter machining times.

This research goes in the direction of efficient spiral bevel manufacturing using universal multitasking machines or five-axis milling centers, where the main objective is to further reduce machining time. To this end, the proposed research aims at the semi-finishing stage using highly efficient double-flank machining where not only the path of the tool, but also the shape of the tool itself are the unknowns in an optimization-based framework.
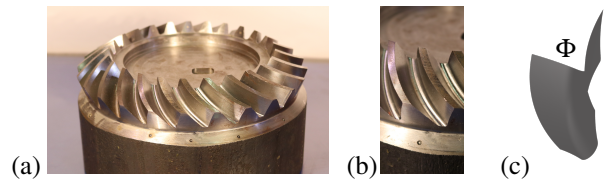

Figure 1: (a) Spiral bevel gear (5-axis CNC machined using the proposed methodology). (b) A zoom-in to one tooth space (aka "valley") between two teeth and its CAD model that is formed by a doubly curved free-form surface Φ (c).

The rest of the paper is organized as follows. Section 3 gives a brief summary of the mathematical derivation of the custom-shaped tool design and its 3D motion. Section 4 describes the case study and Section 5 shows the results obtained. Finally, Section 6 discusses the future research directions and concludes the paper.

3. Double-flank machining and custom-shaped tool design

The basic building blocks of the double-flank machining algorithm will be briefly recalled, more details can be found in [11]. The proposed approach first initializes the motion of the tool using a bisector surface of the tooth space and estimates the initial shape of the tool (Section 3.1), followed by global tool and motion optimization (Section 3.2).
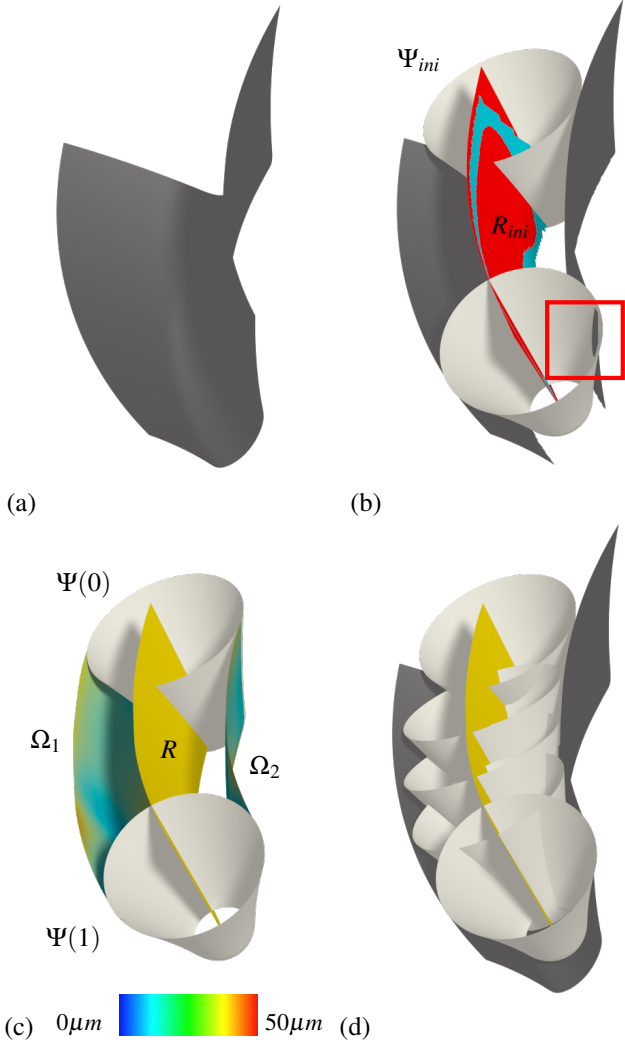
Figure 2: Design of the custom-shaped tool. (a) A cavity bewteen two teeth represented as a spline surface. (b) The self-bisector B (blue) is fitted by a ruled surface R_{ini} (red) and an initial shape, Ψ_{ini}, of the tool is computed. The initial tool and its initial position may penetrate the reference surface (framed in red). (c) The tool Ψ and its trajectory R both undergo global optimization to minimize the error of the left (Ω_1) and right (Ω_2) envelopes from Φ. The envelopes are color-coded by the distance error dist($\Phi_i - \Omega_i$), $i = 1, 2$, that meets fine machining tolerance of $50\mu m$. (d) The final double-flank motion of the custom-shaped tool Ψ through the gear valley.

3.1. Initialization of double flank machining

The goal is to approximate the space between two teeth of a gear Φ, recall Fig. 1, by an *envelope* of a general tool Ψ such that there is a bi-tangential contact between Φ and Ψ on both sides of the tooth space (double-flank machining). The unknowns in an optimization-based algorithm are both the machining tool Ψ and a ruled surface R (the motion of the tool's axis). The ruled surface is represented as a (3×1)-tensor product B-spline patch

$$R(t,s) = (1-s)\mathbf{p}(t) + s\mathbf{q}(t), \quad [t,s] \in [0,1] \times [0,1], \quad (1)$$

where s is the parameter in the direction of rulings and t is the time parameter of the two boundary cubic B-spline curves $\mathbf{p}(t)$ and $\mathbf{q}(t)$, for more details see [11].

Given the valley Φ between two teeth of a gear, first the bottom part of the valley is trimmed off (as this part cannot be flank-machined anyway). This trimming operation defines two side surfaces Φ_1 and Φ_2. As the machining tool is aimed to have tangential contact with both Φ_1 and Φ_2, the bisector surface B is computed. The bisector, however, is a general surface, and therefore spline fitting method is used to compute its ruled surface approximation, see Fig. 2(b).

The initial ruled surface defines the initial shape of the machining tool Ψ and its envelopes define the initial approximation of the two surfaces Φ_1 and Φ_2. The two (right and left) envelopes Ω_1 and Ω_2 are required to approximate Φ_1 and Φ_2, respectively, as close as possible, and within the given machining accuracy $\varepsilon = 50\mu m$, see Fig. 2(c).

To compute the best envelopes Ω_1 and Ω_2, it is formulated as an optimization problem. The unknowns are the two curves $\mathbf{p}(t)$ and $\mathbf{q}(t)$ (boundaries of the rule surface R) and a scalar function $d(s)$ that determines the sphere radius in the ruling direction s. To compute the self-bisector B of Φ, the motion of the tool is conceptualized as a two parameter family of spheres (one in time, second in the ruling direction) that should ideally touch Φ on two sides, see Fig. 2(b). B is then a locus of all such centers of spheres. The right and left sides (defined by trimming off the bottom part of the valley) surfaces Φ_1 and Φ_2 are used, see Fig. 2(b), to compute B, and then

$$F(\mathbf{z}) = \text{dist}(\mathbf{z}, \Phi_1) - \text{dist}(\mathbf{z}, \Phi_2), \quad (2)$$

where $\mathbf{z} \in \mathbb{R}^3$ is the desired center of the sphere and dist is the point-surface minimal distance. The iso-surface $F(\mathbf{z}) = 0$ that defines the bisector B is computed using a variant of the marching cubes algorithm, see [11] for more details.

3.2. Tool and motion optimization

In the proposed optimization-based framework, both the tool Ψ and its motion, represented by a ruled surface R, are optimized. The optimization has two main objectives: (i) to approximate the surface within a fine machining error, i.e, remove as much material as possible and (ii) to guarantee that the envelope of the tool lies inside the valley Φ, i.e., there is no overcut.

As discussed in Section 3.1, an initial ruled surface R^{ini} is computed from the self-bisector B. This gives also, for each value of s, $s \in [0,1]$, a set of scalar values that correspond to the distance dist($R(t,s), \Phi$) and by averaging these values for various t one obtains an initial *radial function* $d^{\star}(s)$. This gives an initial pair of envelopes Ω_1^{ini} and Ω_2^{ini}. However, these envelopes, in general, intersect Φ which corresponds to overcutting, see Fig. 2(b).

To eliminate this phenomenon, the tool Ψ_{ini} and its motion R^{ini} both undergo global optimization. The goal is to optimize them such that Ω_1^{ini} and Ω_2^{ini} become as close as possible to Φ (remove as much material as possible) and they both lie inside the valley (no overcut). To achieve this goal, we proceed as follows. The ruled surface R is uniformly sampled both in t and s parametric directions to obtain $\mathbf{r}_{ij} := R(t_i, s_j), i = 1, \ldots, m, j = 1, \ldots, n$. In our discrete approach, for each s-parameter value (fixed j), one obtains a set of discrete values d_{ij} which are the

3

distances from Φ for a fixed point of the axis as it moves in time. To obtain a motion of Ψ that is penetration-free with Φ (no overcut), we define

$$\underline{d}_j = \min_{i=1,\ldots,m} d_{ij}, \qquad (3)$$

where $\underline{d}_j$ are the penetration-free radii. In this discrete setup, the penetration-free radius depends on the sampling density. $m = 100$ was set in all the experiments; this value turned out to be sufficiently large to return stable values for the valley shown in Fig. 1.

These radii are the lower bounds of the point-surface distance for each j, i.e., distances that define (discrete) radial function that corresponds to a penetration-free tool, see Fig. 2(d). Consequently, the penetration-free error is defined as

$$\varepsilon_j = d_j^\star - \underline{d}_j \qquad (4)$$

where $d_j^\star$ are the samples of the initial radial function $d^\star$. Denote by $\mathbf{d}$ a vector of unknown distances $\mathbf{d} := (d_1, \ldots, d_n)$ and optimize both, the ruled surface R and $\mathbf{d}$.

Finally, the objective that at every time instant t the tool is required to be as close as possible to Φ, but also penetration-free, is formulated. This leads to a minimization problem

$$F_{\mathrm{prox}}(\mathbf{p}, \mathbf{q}, \mathbf{d}) = \frac{1}{mn} \sum_{j=1}^{n} \sum_{i=1}^{m} (\mathrm{dist}(\mathbf{r}_{ij}, \Phi) - d_j - \varepsilon_j)^2 \to \min \quad (5)$$

subject to the axis-rigidity constraints

$$F_{\mathrm{rigid}}(\mathbf{p}, \mathbf{q}) = \langle \mathbf{p}(t_i) - \mathbf{q}(t_i), \mathbf{p}(t_i) - \mathbf{q}(t_i) \rangle - L^2 = 0, \quad (6)$$

where $\mathrm{dist}(,)$ is a point-surface distance and L is the length of $\mathbf{l}$. The unknowns in the minimization are the control points of the two B-spline curves $\mathbf{p}(t)$ and $\mathbf{q}(t)$, and the vector of sphere radii $\mathbf{d}$. $m = 100$ and $n = 30$ was set in the numerical simulations. More details on the whole tool-optimization procedure can be found in [11].

4. Case study

The results of the path-planning algorithm described in [11] were converted into a CL-file, and consequently converted into a G-code, and tested in a conventional machining center, Kondia HS1000, see Fig 3. The semifinishing operations were carried out with both a ball-end tool and a custom-shaped tool. The custom-shaped tool was capable of bitangential machining, which resulted in a simultaneous semifinishing of both walls of the tooth space. One of the objectives was to reduce machining times in the semifinishing stage as the custom-shaped tool admits wide strips of high accuracy and therefore only a single path is needed, in contrast to ball-end milling which requires many milling paths.

Spiral bevel gear was selected as a case study as it is one of the most widespread components in the industrial sector. It is also the element par excellence used to transfer power from one element to another, by transmitting circular motion in terms

of the gear wheel contact. One of the most important applications of gears is the transmission of movement from the shaft of a power source, such as an internal combustion engine or an electric motor, to another, end-effector, shaft. In either case, a high accuracy is highly demanded as the machining errors influence significantly the performance.

The gear wheels can be manufactured from a wide variety of materials to obtain the right mechanical properties. From the point of view of mechanical design, strength and durability, i.e., wear resistance, are the most important attributes. In general, the gear designer should consider the ability to manufacture the gear, from the formation of the gear teeth up to the final assembly of the gear in a machine. Other considerations include weight, corrosion resistance, noise, and cost. F-1550 steel (18CrMo4) was selected as the testing material for manufacturing of the spiral bevel gear, since it reaches a fairly good agreement with all the characteristics that steel needs to possess. Mechanical and physical properties and chemical composition of the used materials are shown in Table 1.

This particular spiral bevel gear was chosen, because its contact surface is larger compared to those of straight-toothed bevel gears, and this fact poses a great challenge when computing both the tool geometry and the machining path. The specific characteristics of the wheel and the theoretical mating pinion for a 5/3 gear ratio are shown in Table 2.

The tests were carried out on a conventional machining center, Kondia HS1000. This machine is a 5-axis milling machine, with 3 linear and 2 are rotary axes. The linear axes are 2 in the head (X, Z) and one in the table (Y), while both rotary axes are in the indexing table (A, C). The spindle speed capacity is 24,000 rpm.

Initially a 210 mm diameter and 120 mm thick steel billet was used as a starting point. A series of previous operations were carried out to achieve a geometry close to the final. These operations are shown in Fig. 4 together with machining times needed for each particular machining stage.

4.1. Custom-shaped tool for SAM

Regarding the SAM tool, a custom-shaped tool was used to perform the semifinishing operation of the tooth space. Its coat was a monolayer electroplated CBN grinding with a grain size of 300 μm, see Figure 5. A tool of this type was chosen due to its excellent tool wear characteristics, because the abrasive grains are resharpened as they break up during the machining process and also because the SAM process is well adapted to the calculation and manufacturing of a custom-shaped tool. When manufacturing the tool core, the thickness of the binding material and the abrasive grains were taken into account in order to obtain a tool with the exact geometry calculated in the modeling stage. The radius of the tool varies from 4.8 mm to 13.2 mm, see Figure 6, and the thickness of the abrasive coat is 0.5 mm. Note that the tool has negative Gaussian curvature (i.e., it is not a conical tool), see [11] for more detailed analysis on the tool design.

Concerning cutting conditions, these were adapted towards the SAM technology in this sort of machining centers, in particular they were adjusted to the spindle capacities, with a spindle
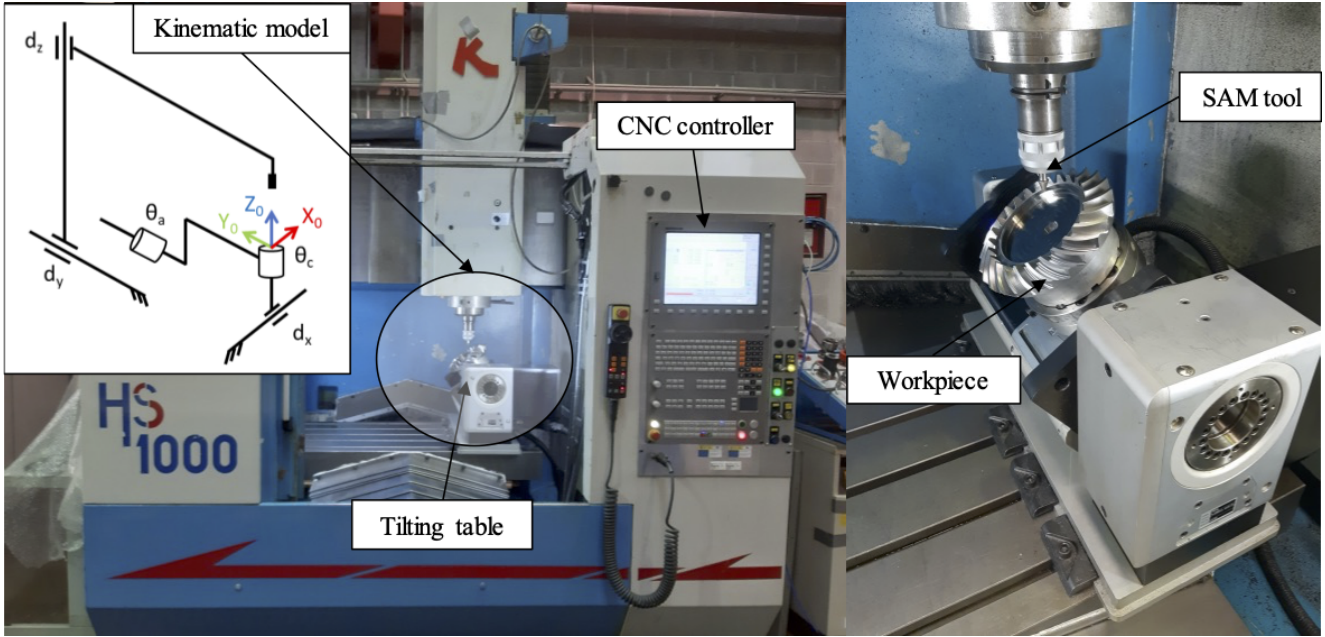
Figure 3: 5-axis milling center.

Table 1: Top: F-1550 steel (18CrMo4) chemical composition (%). Bottom: Mechanical and physical properties. The data are courtesy of [30].

C	Si	Mn	P_{max}	S_{max}	Cr	Mo	Cu_{max}
0.15-0.21	0.15-0.40	0.60-0.90	0.025	0.035	0.90-1.20	0.15-0.25	0.40

Hardness	Yield point	Tensile Strength	Density
34HRC	0.88GPa	1.08GPa	7850 kg/m^3

Table 2: Parameters of a spiral bevel gear.

	Pinion	Gear
Number of teeth	15	25
Outside diameter	124.56mm	207.60mm
Pitch angle	69.4976°	20.5204°
Handedness	Right	Left
Spiral angle β	35°	
Pressure angle α	20°	
Face angle	59.5°	
Shaft angle	90°	
Machining method	Generated	

speed of 24,000 rpm, the limit of the machine, and a feed rate of 250 mm/min. It is important to note the effect of cutting speed on machining, especially in the context of super abrasive machining. The optimal SAM conditions of the speed of rotation should be around 60,000-90,000 revolutions [31]. However, to achieve these speeds, high performance heads are required which conventional machines do not have.

5. Results and validation

To physically validate the results of the modeling algorithm, the machining path of the custom-shaped tool in the manufacturing of a spiral bevel gear was applied. More specifically,

the custom-shaped tool was used in the semifinishing operation, which is the place where Super Abrasive Machining technology has its potential niche of work. In Figure 7, the valley between spiral bevel gear teeth is shown during roughing and semifinishing operations with milling and SAM operations. Observe a clearly visible difference in the quality of surface smoothness in Figure 7(a) and (c).

A qualitative comparison between double-flank machining using a custom-shaped tool and ball end milling, during the semifinishing stage, is presented. Moreover, a virtual comparison against single-flank milling using a barrel tool is also made. In particular, it is shown that surface roughness and manufacturing time are significantly reduced when using double-flank machining with the custom-shaped tool.

5.1. Surface Roughness

Surface roughness is one of the key parameters that influence a smooth movement between gears, their face-face contact, and consequently the life of the whole gear. Typically, the surface roughness is measured using a confocal microscope, however, due to the difficult accessibility of the faces of the gear, resin was applied in order to measure a negative of the tooth space.

The process for obtaining the negative of the face proceeds as follows: first, the area to be measured is degreased with the
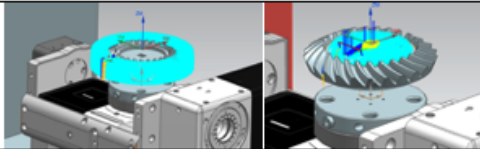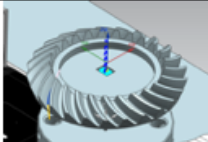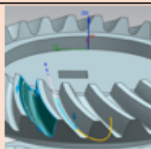
5
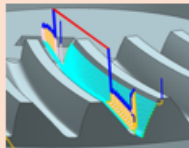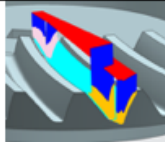
Manufacturing operations	Machining time	CAM trajectories	Progress status
0. Blank	-	-	
1. Preparation of general gear geometry	2:19:00		
2. Refence pocket milling	0:01:14		
3. Roughing gear teeth	2:31:18		
4. Semifinishing gear teeth	-		-
Option A Ball-end milling (conventional)	0:52:55		
Option B SAM (novelty)	0:10:00		
5. Finishing gear teeth	3:07:30		

Figure 4: Progress and machining time summary of the whole gear manufacturing process. The machining time is formatted as hours:minutes:seconds.
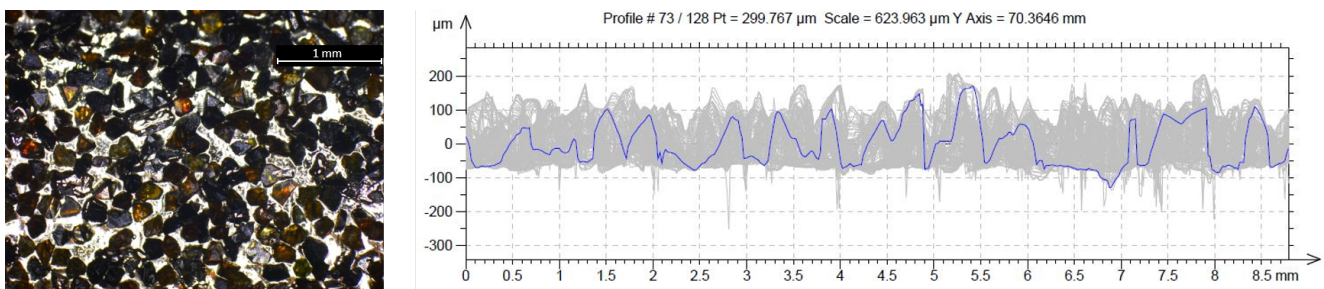

Figure 5: Grain distribution and profile.

DN1 degreaser cleaner provided by PLASTIFORM's own company (PLASTIFORM, Madrid, Spain). Once this is done, a closed area must be formed such that the fluid (liquid resin) covers both sides of the cavity, and then the fluid is applied to the measuring area using a dispensing gun. Finally, cca 6 minutes is needed for the solution to dry out, and then one can remove the negative of the cavity, see Fig. 8.

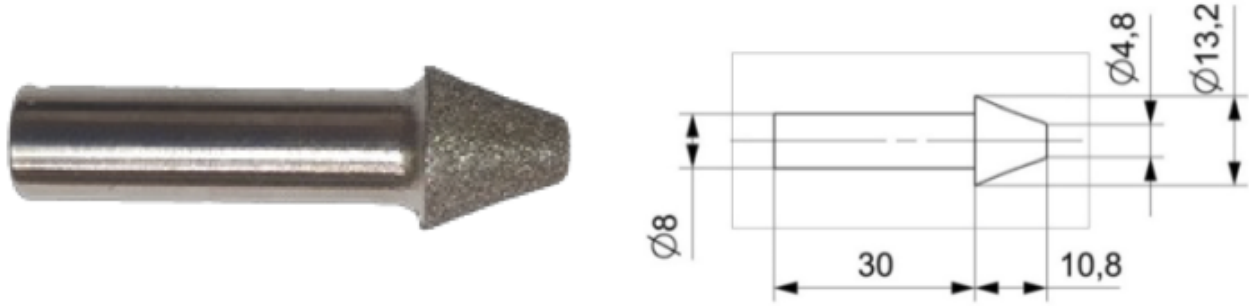It was selected a fluid type resin, so that it could flow through

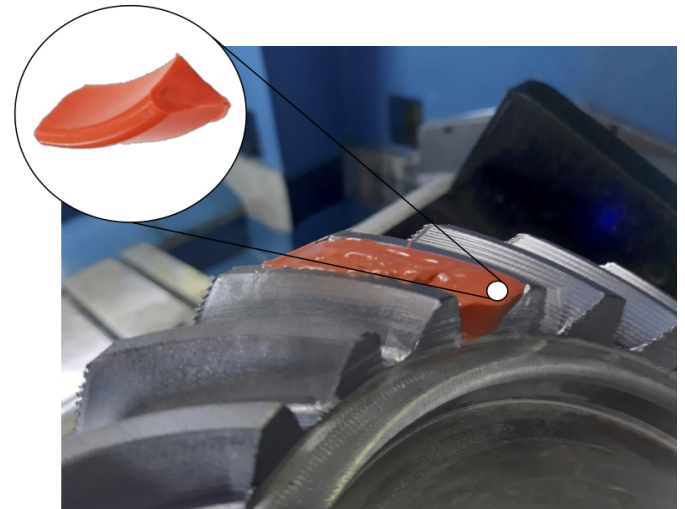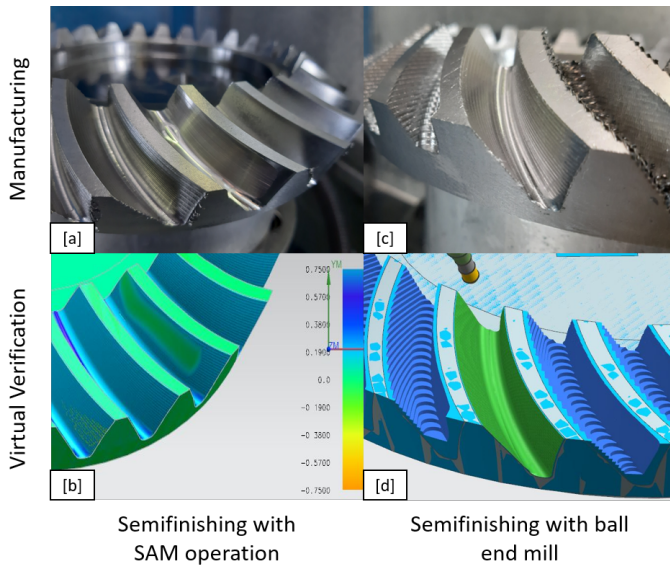Figure 6: Custom-shaped grinding tool and its geometry.

Figure 7: Spiral bevel gear semifinishing operation. (a) Manufacturing with SAM. (b) Virtual verification with SAM. (c) Manufacturing with ball end mill. (d) Virtual verification with ball end mill.

Figure 8: Curing process of the resin and its zoomed-in part after hardening.

the entire gear cavity and thus adapt well to the surface of the faces. Specifically, the F65 product was used, which allows a semi-flexible geometry to be obtained, suitable for measurement by both contact measuring systems and optical measurement systems. The precision obtained with this resin is $\pm 1 \mu m$.

A Leica DCM 3D confocal microscope was used to analyze the surface roughness of the resin. Both sides of the cavity were analyzed, as the amount of excess of material was slightly different on each side after roughing. The adjustment of the roughness measurement in this case was a cutting length of 0.8 mm and an evaluation length of 4 mm, according to ISO 4288 [32]. Figure 9 shows the topography and related data of both sides of the cavity.

Topography on both sides of the tooth cavity shows a perfectly recognizable grinding pattern, in which there are remarked peaks and valleys along the scanned surface caused by the random distribution of the abrasive grains. It is noticeable that slightly better results in term of roughness were obtained on the

right face, as the roughing operation leaves that face smoother and stepless between passes, just the opposite of the left face, as it can be seen in Figure 7(d). However, this fact is not a limitation of the proposed double-flank aproach, but it is due to the fact that the roughing stage left the right face smoother.

The resutls are in accordance with "indicative surface roughness comparison" that many companies handle [33]. The roughness values obtained were acceptable for a semifinishing operation because they are close to those obtained with similar strategies considering them as finishing operations.

5.2. Machining Time

Another aspect that was considered in this work was the analysis of machining time during semifinishing operations on gear teeth. To this end, machining time of ball end milling operation and double-flank SAM strategy with a custom-shaped tool was measured, and barrel flank milling virtual machining time was calculated. The conventional semifinishing operation using a ball end mill with 4 mm diameter was used with a stepover of 0.33 mm of depth of cut in 3 lateral steps in each face and a feed of 2800 mm/min. On the left face, 20 axial passes were repeated 3 times axially (60 passes total) while on the right face
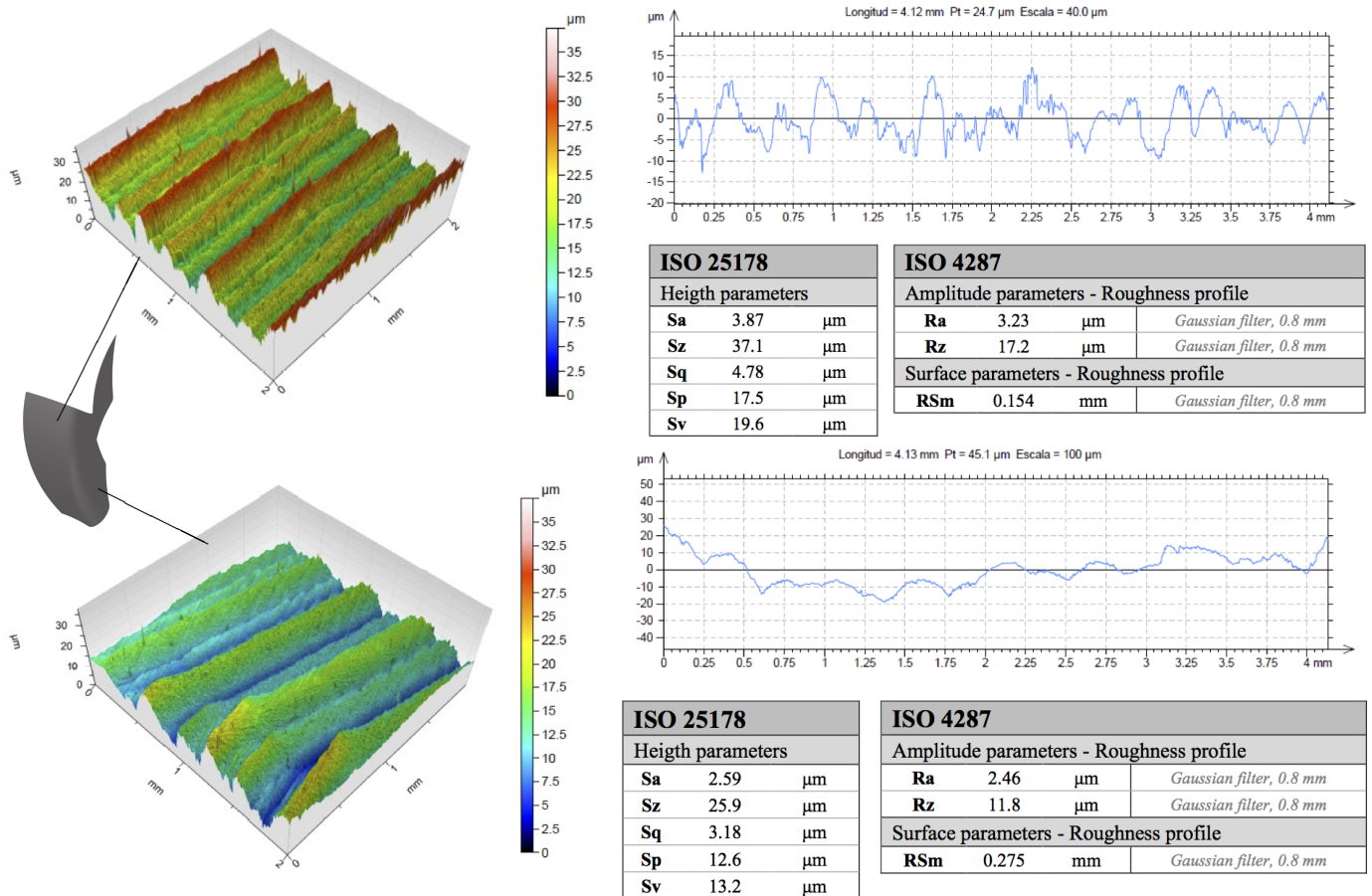
7

Figure 9: Surface area and profile roughness parameters values of the left (top) and right (bottom) side of the gear tooth cavity.

20 passes were sufficient. In contrast, semifinishing using a custom-shaped tool was accomplished in a single sweep with the following parameters: a feed of 500 mm/min and a spindle speed of 16000 rpm. In the case of single flank milling using a barrel-shaped tool with 12 mm of barrel diameter, in total 20 passes were done to cover the whole surface with a feed of 848 mm/min.

With the above-mentioned values of cutting parameters for the three manufacturing semifinishing operations, the following machining time results were obtained: (i) conventional ball end milling: 2 minutes and 7 seconds, (ii) double-flank SAM semifinishing with the custom-shaped tool: 24 seconds, and (iii) barrel flank milling: 1 minute and 8 seconds. Double-flank SAM dominated in terms of machining time. When comparing with the other two, in the case of ball end milling, the semifinishing machining time was reduced by 81.1%, saving in total 43 minutes per gear. In the case of barrel flank milling, SAM double-flank machining was 2.83 times faster than barrel flank milling. See Figure 4 for the summary of the machining times of each particular stage.

5.3. Dimensional Deviation

Dimensional deviation of the three tested semi-finishing strategies: ball end mill operation, double-flank SAM with a custom-shaped tool, and barrel flank milling were qualitatively compared. Figure 10 shows simulation results of the three semifinishing operations using a commercial software.

In the case of the root surface of the tooth, the results obtained by all methods were very similar, reaching a tooth surface excess of material of up to 0.8 mm. The results obtained on the tooth face surface show clear differences. In the case of ball finishing operation, a uniform finish was obtained along the entire surface with a stock around 0.23 mm. In the case of the SAM, there are two clearly differentiated zones. In the first zone, the right face, the values obtained in the semi-finishing are practically close to the final geometry of the piece. On the left side, an undercut of 0.1mm was obtained along the tooth face. Comparing the above-mentioned results with barrel flank milling, it can be seen that the problem on the root surface is almost solved, except for the fillet radius, where is a stock of more than 0.3 mm. However, in the rest of the surface there is an undulation profile that goes from 0.03 mm in the bottom to 0.21 mm in the peak.

5.4. Discussion and Limitations

The proposed approach significantly reduces the semifinishing time by using a properly designed custom-shaped tool. The tool has to be manufactured in advance, however, the custom-shaped tool costs are low, in particular: cylindrical steel bar F115 (85€) to create 4 SAM tools, i.e. 21.25€ per the steel
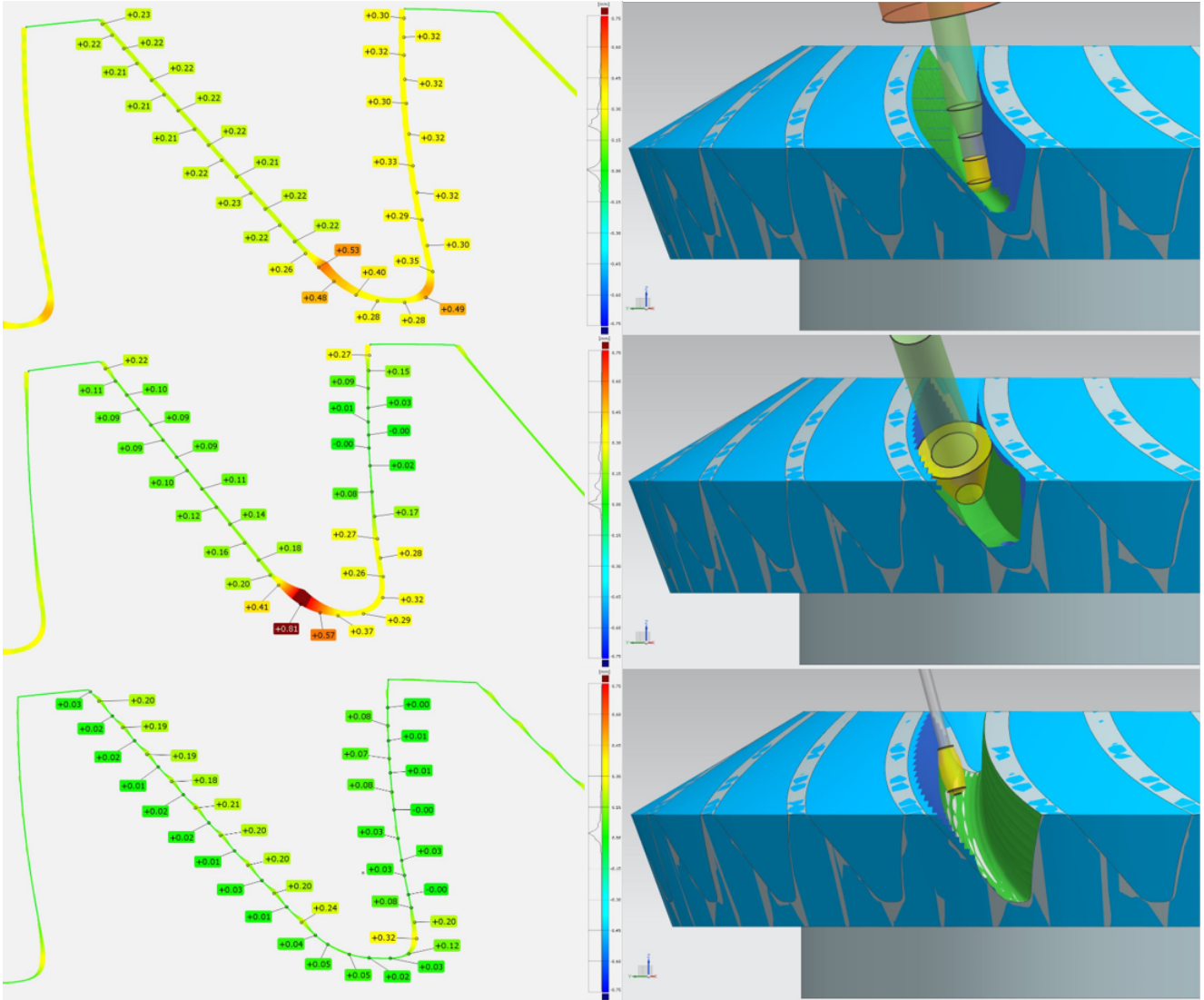
Figure 10: Dimensional deviation of the three virtually simulated semi-finishing strategies: Ball end mill operation (top), double-flank SAM with a custom-shaped tool (middle), and barrel flank milling (bottom). The error distribution along the tooth space (left column) and the simulated paths (right column) are shown.

core of the tool, and 45€ to add the abrasive grains. In total, the cost of the custom-shaped tool is 66.25€. In contrast, the on-market tool for ball end milling, VF4SVBR0200, costs 120€.

The surface roughness values range Sa=2.59-3.87 mm using the SAM approach which is a slightly more than the numbers that can be obtained by means of conventional milling [33]. Nevertheless, these values are acceptable in the case of a workpiece which later undergoes finishing operations.

Another slight limitation is that the very bottom of the cavity is not accessible with the tool whose shape is designed to double-flank the two faces of the cavity. The bottom of the cavity has to be machined using ball end milling approach.

Comparing SAM double-flank machining with flank milling with barrel tools, both approaches offer similar accuracy, but double-flank machining is faster (factor of 2.83) due to the fact that only a single sweep of the tool is needed.

The presented results are promising, however, the double-flank methodology has been tested on one specific type of a

spiral bevel gear, with parameters shown in Table 2. For gears with flat (planar) teeth, the double-flank approach is not challenging as the ideal motion boils down to a plane-plane bisector computation. The other extreme of small and even more curved reference geometry such as, e.g., pinions has not been experimented with, but can be a promising venue for future research.

6. Conclusion and Future Work

We have presented a new variant of 5-axis flank machining, called double-flank. In this machining methodology, not only the machining path, but also the shape of the tool itself are the unknowns in an optimization-based framework. The numerical simulations received in [11] have been validated by physical manufacturing of a steel spiral bevel gear. A custom-shaped SAM tool was designed and created for this purpose and applied in the semifinishing stage. The physical results confirmed the results obtained in the simulation stage, namely that the ma-

chining error gets reduced, the surface roughness is within a standard range, and most remarkably, the machining time of the semifishing stage is reduced by order of magnitude when compared to ball end milling. When compared to flank milling with a barrel tool, the machining time is reduced by factor 2.83. These are very promising results towards future development of double-flank machining as a standard manufacturing technology.

As a future research we aim to further develop this methodology and focus on other geometries, e.g., blades and screw rotors, that seem to be well-suited for double-flank milling methodology using custom-shaped tools. Another research thread can go towards milling as the concept of double-flank methodology is not limited only to abrasive tools, but could also be used for cutting tools with flutes.

References

[1] W. Krumme. *Klingelnberg–Spiralkegdräder (Klingelnberg Spiral Bevel Gears) (in German)*. Springer, 1967.

[2] Zhenyu Zhang, Yaxing Song, Chaoge Xu, and Dongming Guo. A novel model for undeformed nanometer chips of soft-brittle hgcdte films induced by ultrafine diamond grits. *Scripta Materialia*, 67(2):197–200, 2012.

[3] Alfonso Fuentes-Aznar, Ramon Ruiz-Orzaez, and Ignacio Gonzalez-Perez. Numerical approach for determination of rough-cutting machine-tool settings for fixed-setting face-milled spiral bevel gears. *Mechanism and Machine Theory*, 112:22–42, 2017.

[4] Hermann J Stadtfeld. *Gleason Bevel Gear Technology: The Science of Gear Engineering and Modern Manufacturing Methods for Angular Transmissions*. Gleason Works, 2014.

[5] Henry John Watson. *Modern gear production*. Elsevier, 2013.

[6] Xiao-zhong Deng, Geng-geng Li, Bing-yang Wei, and Jing Deng. Face-milling spiral bevel gear tooth surfaces by application of 5-axis CNC machine tool. *The International Journal of Advanced Manufacturing Technology*, 71(5-8):1049–1057, 2014.

[7] Álvaro Álvarez, Amaia Calleja, Naiara Ortega, and Luis de Lacalle. Five-axis milling of large spiral bevel gears: toolpath definition, finishing, and shape errors. *Metals*, 8(5):353, 2018.

[8] SH Suh, WS Jih, HD Hong, and DH Chung. Sculptured surface machining of spiral bevel gears with CNC milling. *International Journal of Machine Tools and Manufacture*, 41(6):833–850, 2001.

[9] Ian Gibson, David W Rosen, Brent Stucker, et al. *Additive manufacturing technologies*, volume 17. Springer, 2014.

[10] Pengbo Bo and Michael Bartoň. On initialization of milling paths for 5-axis flank CNC machining of free-form surfaces with general milling tools. *Computer Aided Geometric Design*, 71:30–42, 2019.

[11] Pengbo Bo, Haizea González, Amaia Calleja, Luis Norberto López de Lacalle, and Michael Bartoň. 5-axis double-flank CNC machining of spiral bevel gears via custom-shaped milling toolspart I: Modeling and simulation. *Precision Engineering*, 62:204–212, 2020.

[12] Jinesh Machchhar, Denys Plakhotnik, and Gershon Elber. Precise algebraic-based swept volumes for arbitrary free-form shaped tools towards multi-axis CNC machining verification. *Computer-Aided Design*, 2017.

[13] Pengbo Bo, Michael Bartoň, Denys Plakhotnik, and Helmut Pottmann. Towards efficient 5-axis flank CNC machining of free-form surfaces via fitting envelopes of surfaces of revolution. *Computer-Aided Design*, 79:1–11, 2016.

[14] C. Li, S. Bedi, and S. Mann. Flank millable surface design with conical and barrel tools. *Computer- Aided Design and Applications*, 5:461–470, 2008.

[15] Zhenyu Zhang, Siling Huang, Shaochen Wang, Bo Wang, Qian Bai, Bi Zhang, Renke Kang, and Dongming Guo. A novel approach of high-performance grinding using developed diamond wheels. *The International Journal of Advanced Manufacturing Technology*, 91(9):3315–3326, 2017.

[16] Zhenyu Zhang, Junfeng Cui, Bo Wang, Ziguang Wang, Renke Kang, and Dongming Guo. A novel approach of mechanical chemical grinding. *Journal of Alloys and Compounds*, 726:514–524, 2017.

[17] Zhenyu Zhang, Fengwei Huo, Xianzhong Zhang, and Dongming Guo. Fabrication and size prediction of crystalline nanoparticles of silicon induced by nanogrinding with ultrafine diamond grits. *Scripta Materialia*, 67(7-8):657–660, 2012.

[18] Zhenyu Zhang, Dongming Guo, Bo Wang, Renke Kang, and Bi Zhang. A novel approach of high speed scratching on silicon wafers at nanoscale depths of cut. *Scientific Reports*, 5(1):1–9, 2015.

[19] Zhenyu Zhang, Bo Wang, Renke Kang, Bi Zhang, and Dongming Guo. Changes in surface layer of silicon wafers from diamond scratching. *Cirp Annals*, 64(1):349–352, 2015.

[20] Faydor L Litvin and Alfonso Fuentes. *Gear geometry and applied theory*. Cambridge University Press, 2004.

[21] Hartmuth Müller and Joachim Thomas. Face-off: face hobbing vs. face milling. *Gear Solutions*, 5(54):49–60, 2007.

[22] Fritz Klocke, Markus Brumm, and Julian Staudt. Quality and surface of gears manufactured by free form milling with standard tools. In *Proceedings of the International Gear Conference, Lyon, France*, pages 26–28, 2014.

[23] Álvaro Álvarez, Amaia Calleja, Naiara Ortega, and Luis de Lacalle. Five-axis milling of large spiral bevel gears: toolpath definition, finishing, and shape errors. *Metals*, 8(5):353, 2018.

[24] Wuhao Zhuang, Lin Hua, Xinghui Han, and Fangyan Zheng. Design and hot forging manufacturing of non-circular spur bevel gear. *International Journal of Mechanical Sciences*, 133:129–146, 2017.

[25] Álvaro Álvarez, Amaia Calleja, Mikel Arizmendi, Haizea González, and Luis Lopez de Lacalle. Spiral bevel gears face roughness prediction produced by CNC end milling centers. *Materials*, 11(8):1301, 2018.

[26] Xiao-yu Yang and Jin-yuan Tang. Research on manufacturing method of CNC plunge milling for spur face-gear. *Journal of Materials Processing Technology*, 214(12):3013–3019, 2014.

[27] Fritz Klocke, Markus Brumm, and Julian Staudt. Quality and surface of gears manufactured by free form milling with standard tools. In *Proceedings of the International Gear Conference, Lyon, France*, pages 26–28, 2014.

[28] Włodzimierz Wilk and Jacek Tota. Modern technology of the turbine blades removal machining. In *Proc. of the* 8th Int. Conf.Advanced manufacturing Operations, Scientific reports*, pages 347–355, 2008.

[29] Haizea González Barrio, Amaia Calleja Ochoa, Octavio Manuel Pereira Neto, Naiara Ortega Rodríguez, Luis Norberto López de Lacalle Marcaide, and Michael Barton. Super abrasive machining of integral rotary components using grinding flank tools. 2018.

[30] Steel Composition. https://virgamet.com/18hgm-18crmo4-1-7243-18cd4-708m20-15crmo4-case-hardening-steel.

[31] DK Aspinwall, SL Soo, DT Curtis, and AL Mantle. Profiled superabrasive grinding wheels for the machining of a nickel based superalloy. *CIRP annals*, 56(1):335–338, 2007.

[32] DIN EN ISO 4288. Geometrical product specifications (gps)surface texture: Profile method: Rules and procedures for the assessment of surface texture. 1996.

[33] Surface finish ranges and tolerances. `https://www.cnccookbook.com/surface-finish-chart-symbols-measure-calculators/`.